

# Investigation of the effective parameters on the phenol removal from the groundwater by response surface method

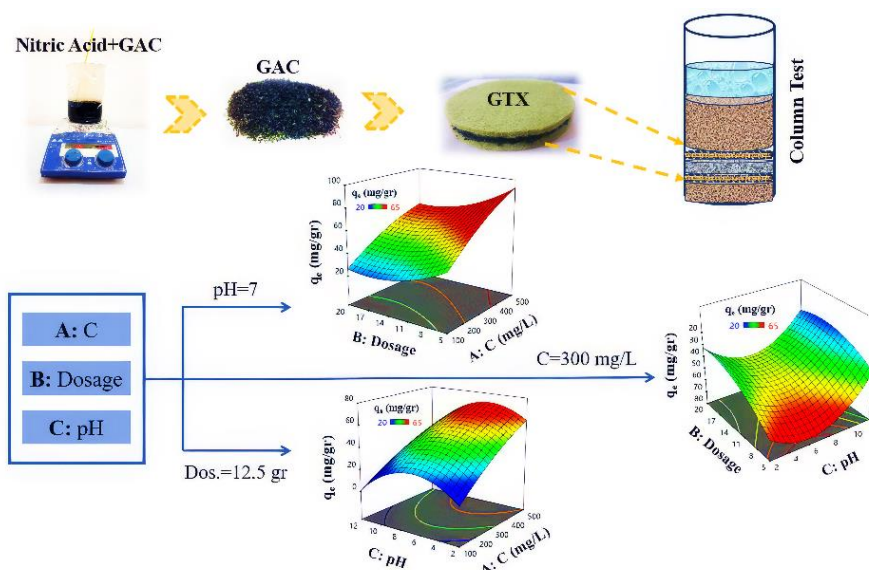
Khatereh Ahmadi<sup>1</sup>, Farhad Qaderi<sup>1,\*</sup> , S. Mostafa Rahmaninezhad<sup>2</sup>, Reza Shidpour<sup>3</sup>

<sup>1</sup>Department of Environmental Engineering, Faculty of Civil Engineering, Babol Noshirvani University of Technology, Babol, Iran.

<sup>2</sup>Department of Civil Engineering, Faculty of Civil Engineering, University of Texas Rio Grande Valley, Texas, USA.

<sup>3</sup>Department Material Engineering, Faculty of Materials and Industrial Engineering, Babol Noshirvani University of Technology, Babol, Iran.

## GRAPHICAL ABSTRACT



## ARTICLE INFO

**Article type:**  
Research Article

**Article history:**  
Received 10 August 2023  
Received in revised form 12 October 2023  
Accepted 14 October 2023  
Available online 16 October 2023

**Keywords:**  
Phenol  
Adsorbent  
Groundwater  
Response surface method

  
© The Author(s)  
Publisher: Razi University

## ABSTRACT

The discharge of industrial waste containing organic pollutants like phenol has caused a surge in environmental complications in water, soil, and air. In recent years, the concentration of phenolic pollutants has risen due to their high toxicity and environmental persistence. This research used geotextile/activated carbon (GTX/AC) adsorbent to purify groundwater contaminated with phenol, owing to its easy availability. A low-cost geotextile carrier was utilized to avoid the dispersion of active carbon in the groundwater. Response surface method (RSM) was used in the present research to design and optimize experimental tests. The results indicate that the initial concentration, pH, and adsorbent dosage are the most significant parameters affecting the geotextile/activated carbon (GTX/AC) adsorbent performance. Maximum adsorption capacity was considered the highest desirability level for the response surface method optimization. The initial phenol concentration equal to 458.8 mg/L, the amount of pH equal to 7, and the dose of adsorbent equal to 5.5 gr were the best conditions for removing phenol from the water. Based on the result of this research, the response surface method can be used for modeling and optimizing phenol adsorption from groundwater, and geotextile/activated carbon (GTX/AC) adsorbent is a suitable choice for the treatment of water polluted with phenol.

## 1. Introduction

Phenols are organic pollutants found in industrial effluents due to their widespread use in industries such as resin, plastic, pharmaceutical, <sup>\*</sup>Corresponding author Email: [F.Qaderi@nit.ac.ir](mailto:F.Qaderi@nit.ac.ir)

dye, and pesticide. These substances are difficult to remove from wastewater and cannot be easily degraded (Han, Zhang, and Wu, 2020). As a result, it is necessary to use effective techniques to treat phenol before discharging industrial effluents into surface and

groundwater streams (Khataei, Mokhtarani, and Ganjidoust, 2017; Sharafi et al., 2019; Khataei, Mokhtarani, Ganjidoust, 2019). Adsorption is an effective method for eliminating organic compounds such as phenol. Adsorbent materials are readily available, cost-effective, and can be reused (Khalatbary et al., 2022). Carbon adsorbents are especially promising for removing phenol from industrial wastewater due to their high porosity and surface area (Abussaud et al., 2016; Guo et al., 2019). Agricultural waste is widely used to produce activated carbon due to its low cost (Mohammadi, Darijani, Karim, 2020). Although Activated carbon (AC) is a commonly used adsorbent, its high regeneration cost limits its application. Additionally, the carbon used for adsorbing organic materials can be brittle, generating carbon fines. Over time, microcarbons cause the turbidity of treated water or wastewater, which leads to more pollution. Nonetheless, it remains challenging to eliminate and retrieve the spent AC powders from water, which leads to further contamination. Electric and magnetic fields cannot control AC powders due to their non-polarity. Centrifugation and filtration are frequently employed to separate used activated carbon powders, but these methods can be costly. Using a suitable cover to carry activated carbon in a water environment can be an effective way to trap, recover and recycle it and prevent secondary pollution after adsorption processes.

Additionally, the RSM method has been widely used in pollutant adsorption research (Nowrouzi and Abyar, 2021). For instance, Arida et al., (2016) conducted research on the using of chitosan-coated bentonite (CCB) for As(V) removal from groundwater in a fixed-bed system (Arida et al., 2016). They used RSM, which corresponds to Box–Behnken design (BBD), to optimize crucial factors, including the amount of adsorbent, flow rate, and inflow concentration. In this context, Koolivand and Shahbaz (2018) studied the adsorption of methylene blue (MB), a commonly used toxic dye, onto graphene oxide (GO) (Koolivand and Shahbazi, 2018). The optimization of batch condition and condition of using a fixed-bed column for adsorption of MB was achieved through using the RSM method (based on BBD). Shanmugaparakash et al., (2018) conducted studies to compare the performance of RSM and Artificial neural networks (ANNs) methods in predicting the adsorption rate of Zn(II) ions (Shanmugaparakash et al., 2018). Moghimi et al., (2020) used Central Composite Design (CCD) as an RSM approach to optimize the adsorption capacity of Sb(III) (Moghimi et al., 2020).

This research used granular activated carbon and a geotextile carrier to remove phenolic pollutants from groundwater. The activated carbon was first acid-washed to increase its porosity and hydrophilicity. Modified activated carbon granules were placed between two geotextile layers to prevent their dispersion in water flow. The response surface method (RSM) was used to investigate the factors affecting phenol adsorption, assess each independent variable's synergistic or reducing effects, and determine the optimal conditions. This research delves into developing an innovative and cost-effective approach to removing phenolic pollutants from groundwater using activated carbon and geotextile carriers. Geotextile was employed as a readily available, affordable, and high-strength material. It was utilized to facilitate the separation of activated carbon from the environment for reuse. This carrier prevents the dispersion of granular activated carbon, which could create turbidity in the water environment. By doing so, it enhances the efficiency of the adsorbent and allows for reuses throughout its lifecycle. The study involved a comprehensive experimental program investigating the effectiveness of granular activated carbon and geotextile carriers as adsorbents for removing phenolic pollutants from groundwater.

**2. Materials and methods**

The intended column is made of PVC plastic cylinders, an Iranian product (inner diameter=10.4 cm; height = 40 cm). It contains a fixed bed of adsorbent and sandy soil. The adsorbent fixed bed comprises coconut shell-based activated carbon granules (produced by Jacobi Company in Japan) with a minimum hardness of 75 and a density ranging from 480 to 510 kg/m<sup>3</sup>, along with a geotextile having a density of 500 g/m<sup>2</sup>. The column's environment consisted of sandy soil with a relative density of 70%. It was treated with 5M nitric acid at 50 °C for 3 hours to make activated carbon hydrophilic and porous. After being washed with distilled water to (neutralize the pH), the samples were dried (80°C). For the test column that contained sandy soil, circular sections with a diameter of 10.4 cm were cut from non-woven polyethylene terephthalate GTXs (GTXs were produced by Geosakht company in Iran). To remove impurities and oil from the surface of the geotextile, the geotextile was washed using distilled water and ethanol in an ultrasonic bath (30 minutes). After that, it was dried in an 80°C oven. 5 M hydrochloric acid and 5 M sodium hydroxide solutions adjusted the pH. The system was initially saturated with distilled water to conduct the column tests. Fig. 1 shows a view of the process. In the

study, the tests were conducted using three variables: phenol concentration, pH, and adsorbent amount, utilizing the RSM method. In this series of tests, the flow rate of pollutants was set at 12.5 mL/min. Phenol concentration in the column output was measured at 270 nm wavelength using a spectrophotometer.

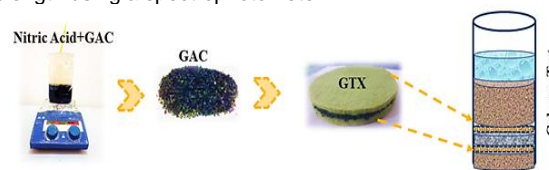


Fig. 1. A schematic view of the adsorbent column in the pilot.

**2.1. Design experiment with RSM**

The RSM method was used to determine optimized conditions for maximum phenol adsorption (the maximum adsorption capacity) in columns containing sandy soil and the adsorbent filter. Design Expert software (version 11) was utilized to carry out the experiment's design. The independent variables were used to design experiments (phenol concentration, pH, adsorbent dosage). This method efficiently analyses the interaction between parameters, mutual effects of independent variables on the maximum phenol adsorption in sandy columns with an adsorbent filter, and optimization of effective parameters. The chosen levels for the experiments were specifically selected to ensure that the research findings could be used to make informed decisions on a field scale and applied in experiments.

The initial concentration range of 100-500 mg/L was selected (for -1 and +1 levels of initial concentration in response surface methodology) due to the outlet of petrochemicals and oil industries in coastal cities. Additionally, the pH range selected was 2-12, with midpoint equal to 7 (for -1, 0 and +1 levels of pH in response surface methodology), to check the pH in acidic, basic, and neutral ranges. The primary objective was to explore the neutral point since the phenol solution typically has a pH of 6.5, near the neutral range. The adsorbent amount range was chosen to be between 5 and 20 grams (for -1 and +1 levels of adsorbent amount in response surface methodology) based on pretests and literature review (Abussaud et al., 2016; Iheanacho et al., 2021; Mandal et al., 2021). Finally, the experiments were designed using different ranges of independent variables; (as Initial concentration (5, 100, 300, 500, 600 mg/L), pH (1, 2, 7, 12, 14), Dosage of adsorbent (1.25, 5, 12.5, 20, 23.75 gr/Lit)). In the present study, using the CCD design, the amount of  $\alpha$  was assumed manually equal to 1.5. The  $-\alpha$  and  $+\alpha$  levels were obtained at 0 and 600 mg/L (for initial concentrations). The value of zero was non-polluting and meaningless, and the number 5.0 mg/L was replaced by it. Also, the  $-\alpha$  level of pH is equal to -0.5, which is not within the reasonable range, and therefore, the value of 1.0 is considered in the present study. In some previous research, manual levels had been used for independent variables to choose suitable applicable ranges for independent variables. It must be mentioned that the base of these calculations can be found in previous research about RSM (Wang, 2006). Regarding the CCD method, the response variable (i.e., maximum phenol adsorption) was related to the independent variables through Eq. 1, as follows:

$$q_{eq}(mg/gr) = \beta_0 + \sum_{i=1}^k \beta_i x_i + \sum_{i=1}^k \beta_{ii} x_i^2 + \sum_{i=1}^k \sum_{j=1}^k \beta_{ij} x_i x_j + \varepsilon \quad (1)$$

where,  $q_{eq}$  is the predicted response,  $\beta_0$  is a constant coefficient,  $\beta_i$  is a linear coefficient,  $\beta_{ii}$  is a quadratic coefficient,  $\beta_{ij}$  is interaction coefficient,  $x_i$  and  $x_j$  are coded values of the variables,  $\varepsilon$  is residual error. Finally, the proposed tests are shown in Table 1.

**3. Results and discussions**

**3.1. Statistical results from RSM model analysis**

Design expert software performed variance analysis (ANOVA) of the experiment results. Statistical results are summarized in Table 1. The F-value and p-values determine the significance level of the proposed model for phenol adsorption capacity in the sand column system with filter adsorbent (Eq. 2). The F-value is a statistical analysis used to assess the relationship between the model and the residual errors. Also, a p-value lower than 0.05 represents the importance of the independent variables, while parameters with a p-value greater than 0.05 are considered non-significant. Results show that the p-value of the adsorption capacity model was less than 0.0001, indicating that the model is significant. According to Table 2, the linear effect of initial concentration (A), the interactive effect between initial concentration and pH, and the square effect of pH are recognized as the most

significant factors for the phenol adsorption capacity. The lack-of-fit was higher than 0.05 for the model equation of phenol adsorption, showing that the quadratic model is appropriate for phenol adsorption from groundwater. The graphs generated from the RSM software were confined within the selected ranges, and the -α and +α levels were not taken into account. The -α and +α levels are typically used to verify the accuracy of the selected ranges. In case the lack of fit value is not significant, it indicates that the ranges are chosen correctly.

**Table 1.** Proposed tests designed by RSM.

Test	A: C, mg/L	B: Ads., g	C: pH	
Main Test	1	100	5	2
	2	500	5	2
	3	100	20	2
	4	500	20	2
	5	100	5	12
	6	500	5	12
	7	100	20	12
	8	500	20	12
Outlier	9	5	12.5	7
	10	600	12.5	7
	11	300	1.25	7
	12	300	23.75	7
	13	300	12.5	1
	14	300	12.5	14
Central Test	15	300	12.5	7
	16	300	12.5	7
	17	300	12.5	7
	18	300	12.5	7
	19	300	12.5	7
	20	300	12.5	7

Different models were studied to determine the best model, including linear, 2FI, quadratic, and cubic models. The best-fit empirical equation, as mentioned in Table 3, was the quadratic model. The quadratic model has the highest correlation with the experimental database ( $R^2=0.9953$ ) among other types of models. Accordingly, Eq. (2) was finally found as the best-fit quadratic equation for the adsorption capacity ( $q_e$ ) as a function of initial concentration (A), adsorbent (B), and pH (C) as follows:

$$q_e = 53.13 + 20.6551 A - 6.89542 B - 4.82121 C - 2.72294 AB - 3.08855 AC + 1.39375 BC - 8.4012 A^2 + 6.3244 B^2 - 14.3798 C^2 \quad (2)$$

The negative and positive coefficients mentioned in Eq. (2) represent antagonistic and synergistic effects of the process parameters, respectively. Previous research has reported similar results (Rout, Bhunia, Dash, 2017). The quadratic model was selected as this research model. The performance of the proposed equation is shown in Fig. 2. Results show that Eq. (2) agrees with the experimental results and can be a suitable model for predicting adsorption capacity. As mentioned in Fig. 2, the coefficient of variation (C.V.) is 3.42%, showing the accuracy and precision of the expected results. Low C.V. shows that experimental and predicted adsorption capacity has little deviation. Additionally, the value of 69.39 for the Adeq precision displays an appropriate signal; since this parameter should be greater than 4.0.

**Table 3.** Summary of the ANOVA.

Source	Sum of Squares	df	Mean Square	F-value	p-value	
Model	9081.48	9	1009.05	452.04	< 0.0001	Significant
A-C	5300.18	1	5300.18	2374.40	< 0.0001	
B-Dosage	594.33	1	594.33	266.25	< 0.0001	
C-pH	262.14	1	262.14	117.43	< 0.0001	
AB	59.32	1	59.32	26.57	0.0004	
AC	76.31	1	76.31	34.19	0.0002	
BC	15.54	1	15.54	6.96	0.0248	
A <sup>2</sup>	702.58	1	702.58	314.74	< 0.0001	
B <sup>2</sup>	408.10	1	408.10	182.82	< 0.0001	
C <sup>2</sup>	1486.33	1	1486.33	665.85	< 0.0001	
Residual	22.32	10	2.23			
Lack of Fit	3.41	5	0.6828	0.1805	0.9582	Not significant
Pure Error	18.91	5	3.78			
Cor Total	9103.81	19				

### 3.2. Individual effect of variables

Fig. 3 shows the individual effect of independent variables on the adsorption capacity. The impact of initial concentration (single variable) on the adsorption capacity is depicted in Fig. 3a. Results demonstrate that as the initial concentration rises from 100 to 500 mg/L, the value of  $q_e$  also goes up. However, for higher initial concentrations ( $C>500$  mg/L), a decrease in the slope was observed. This observation may be attributed to the fact that although increasing the initial concentration increases phenol contact with adsorption sites, the output concentration also increases; therefore, it causes a lower removal percentage. Previous research reported similar results (Chen et al., 2022).

**Table 3.** Efficiency of predicting models for adsorption capacity.

Source	Std. Dev.	R <sup>2</sup>	Adjusted R <sup>2</sup>	Predicted R <sup>2</sup>	PRESS	
Linear	13.36	0.6865	0.6277	0.4912	4631.91	
2FI	14.42	0.7031	0.5661	0.2018	7267.03	
Quadratic	1.49	0.9975	0.9953	0.9932	61.81	Suggested
Cubic	1.94	0.9979	0.9921		*	Aliased

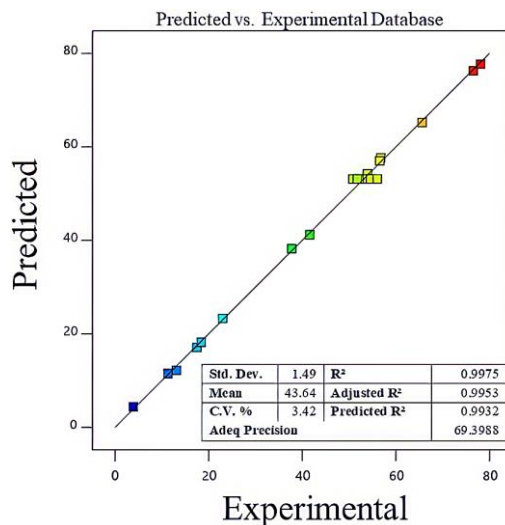


**Fig. 2.** The predicted model (Eq. 2) as compared to the experimental database.

Generally, results show that the maximum value of  $q_e$  was recorded at 500 mg/L. Fig. 3b illustrates the effect of adsorbent dosage, as an independent variable, on the adsorption capacity of the GTX/AC adsorbent. As shown in the Fig. 3b, as the dosage of the adsorbent increases from 5 gr to 16 gr, the  $q_e$  decreases from 67 mg/gr to about 51 mg/gr. However, this trend changed for adsorbent dosages higher than 16 gr; where adsorbent increases from 16 g to 20 g, the  $q_e$  increases from 51 mg/g to about 53 mg/g. Accordingly, results show that the maximum adsorption capacity is 65.3 mg/gr. Moreover, Fig. (3c) clarifies the impact of pH variation on adsorption capacity. As per the results, the column's maximum adsorption capacity is observed at pH=6.35, which aligns with the findings of existing literature on the topic (Beker et al., 2010). An increase in  $q_e$  was observed when the pH of the inlet contaminant solution was increased within the range of 2-6.35. On the other hand, a decrease in  $q_e$  was noticed when the pH was reduced within the range of 6.35 < pH < 12. Thus, in this range, the adsorption capacity of the GTX/AC adsorbent also shows a descending trend. The adsorption capacity reached its lowest level at the pH=12. Moreover, it is worth mentioning that a comparison between the results of the GTX/AC adsorbent-contained column and only the sand-contained column was conducted in the present study. Table 4 summarizes that using novel GTX/AC composite considerably enhanced the phenol adsorption capacity for all cases.

### 3.3. Interaction effects of variables on the adsorption capacity

Interaction effects curves illustrate the impact of independent variables on each other, whether synergistic or antagonistic. They may also indicate that the variables do not significantly affect each other. To determine the interaction effect of independent variables, the changes in the  $q_e$  value are analyzed when the changes occurred in one independent variable (such as concentration) at two different levels of the other independent variable (such as adsorbent dosage). If the slope changes of the  $q_e$  increases while moving from the low level of the variable (Adsorbent dosage=5 gr) to the high level (Adsorbent dosage=20 gr), it indicates that the independent variables have a

synergistic effect on each other, Otherwise, they have an antagonistic effect.

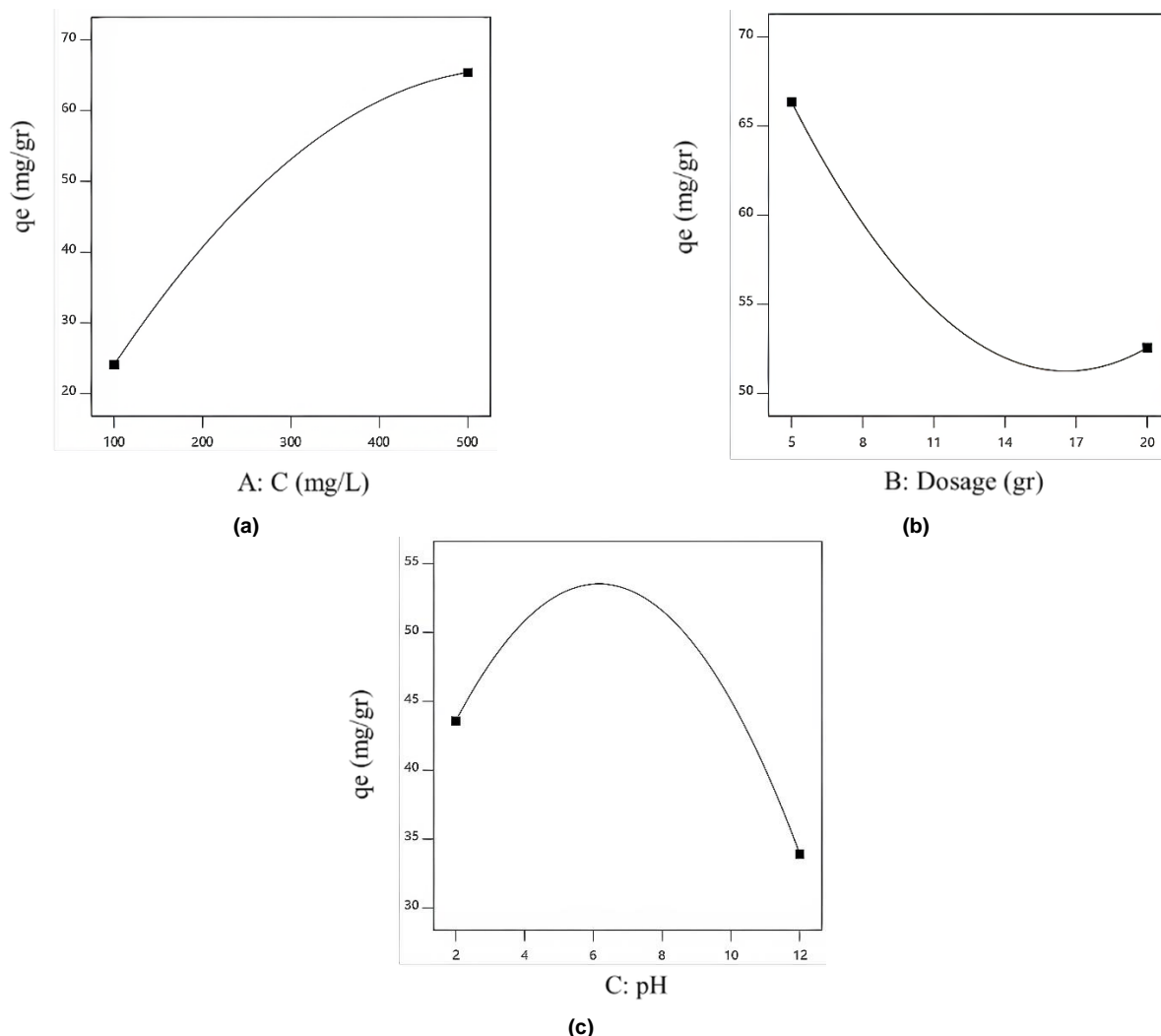


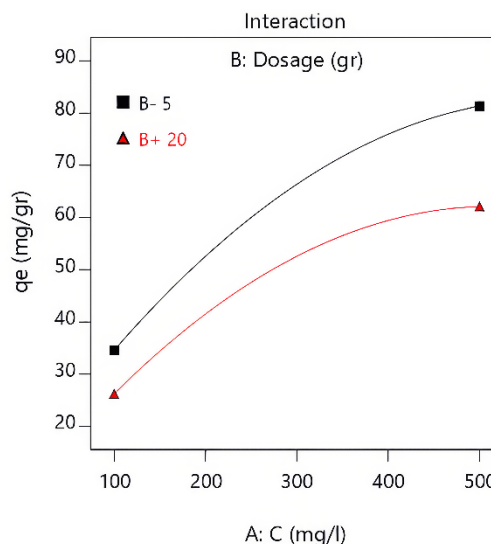
Fig. 3. The individual effect of independent variables (a) concentration; (b) dose of adsorbent; (c) pH.

Table 4. The results of Experiments recommended by CCD in the RSM.

Test	$q_{eq}$ , mg/g		
	Only Sand Value	GTX/AC Value	RSM Predicted Value for GTX/AC
1	0.23	22.98	23.32
2	0.78	76.52	76.25
3	0.14	13.12	12.18
4	0.55	53.90	54.23
5	0.18	17.45	17.06
6	0.58	56.757	57.64
7	0.12	11.29	11.51
8	0.43	41.59	41.19
9	0.04	3.89	4.39
10	0.67	65.60	65.21
11	0.79	78.11	77.70
12	0.58	56.52	57.02
13	0.39	37.75	38.21
14	0.21	18.43	18.20
15	0.52	50.80	53.13
16	0.54	53.77	53.13
17	0.54	52.127	53.13
18	0.53	51.77	53.13
19	0.55	5.54	53.13
20	0.57	56.001	53.13

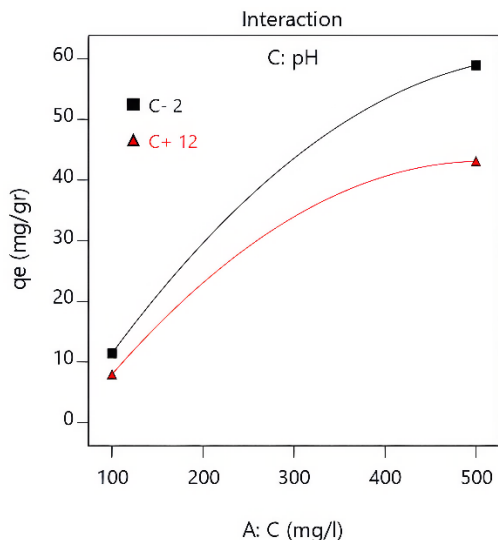
Fig. 4 shows the interaction between the concentration and adsorbent amount. The x-axis shows changes in concentration, and the effect of the adsorbent dosage on the concentration has been investigated by moving from the low level to the high level (Adsorbent dosage =20 gr). Results indicate that the slope changes of  $q_e$  in the lower level of the adsorbent dosage are more significant than the

higher-level one. However, increasing the initial concentration value results in an increasing  $q_e$ , but this increase has a lower slope at a higher level of Adsorbent dosage (Adsorbent dosage =20 gr) compared to a lower level of Adsorbent dosage (Adsorbent dosage =5 gr); therefore, the interaction effect of the adsorbent dosage and initial concentration is antagonistic. When the pollutant concentration and initial concentration increase, the efficacy of using  $q_e$  as an adsorbent tends to decrease. This occurs because the rate of adsorbate increase is relatively lower than the rate of increase of the pollutant concentration. It is worth noting that, while there is an antagonistic relationship between initial concentration and adsorbent dosage, it is not particularly significant.



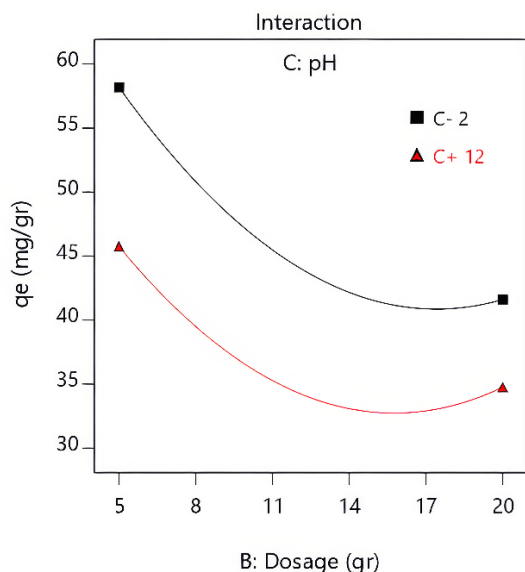
**Fig. 4.** Interaction effect of initial concentration and adsorbent dosage on adsorption capacity.

Fig. 5 shows the interaction effect of phenol's initial concentration and pH. Findings depict that the slope changes of  $q_e$  are higher at a low pH level (pH=2) than at a high level (pH=12). In other words, with the increase of pH from 2 to 12, the value of  $q_e$  decreased. In addition, the rate of increase in  $q_e$  when the initial concentration increased is lower in pH=12 than pH=2. Therefore, the interaction effect between pH and phenol initial concentration is antagonistic. According to Fig. 5, at pH=12, with the increase of phenol's initial concentration of more than 400 mg/L, the  $q_e$  is approximately constant. This is due to the fact that the adsorbent is saturated in phenol at an initial concentration of less than 400 mg/L.



**Fig. 5.** Interaction effect of initial concentration and pH on adsorption capacity.

Fig. 6 shows the interaction effect of adsorbent dosage and pH. Increasing the amount of adsorbent dosage up to 16 grams results in decreasing changes of  $q_e$  at both low and high pH levels (pH=2 and pH=12). According to Fig. 6, in the range of  $5 \text{ gr} \leq \text{adsorbent dosage} \leq 16 \text{ gr}$ , adsorbent dosage and pH do not significantly affect each other; However, with increasing pH level from 2 to 12,  $q_e$  value decreased. In the range of  $16 \text{ gr} \leq \text{adsorbent dosage} \leq 20 \text{ gr}$ , the  $q_e$  increased. In the range of  $16 \text{ gr} \leq \text{adsorbent dosage} \leq 20 \text{ gr}$ , changes of  $q_e$  with increasing adsorbent dosage at a high pH level (pH=12) is more significant than at a low pH level (pH=2). Thus, pH has a synergetic effect on the adsorbent dosage in the  $16 \text{ gr} \leq \text{adsorbent dosage} \leq 20 \text{ gr}$ .



**Fig. 6.** Interaction effect of adsorbent dosage and pH on adsorption capacity.

### 3.4. Simultaneous effects of variables on the adsorption capacity

Simultaneous effects of independent variables on the adsorption capacity are shown in Figs. 7, 8, and 9. These figures determine the most important independent variables regarding the adsorption capacity. Fig. (7) shows that maximum adsorption occurred at highest concentration (500 mg/L) and the lowest adsorbent dosage (5 mg). At low initial concentrations (about 100 mg/L), no significant variation in the  $q_e$  was observed with increasing adsorbent dosage (from 5 to 20 mg); while increasing in initial concentration (from 100 to 500) has a considerable impact on the  $q_e$  at a low adsorbent dosage (about 5 gr). Moreover, the adsorption capacity gradually decreased by increasing the initial concentration (up to 500 mg/L) and increasing the adsorbent dosage (up to 20 gr). Adsorbents with a predetermined number of binding sites tend to get saturated more rapidly at a specific concentration as the concentration of phenol rises. Consequently, the adsorption capacity also increases (Roy, Das, Sengupta, 2017). Hence, initial concentration is more significant than adsorbent dosage when both act simultaneously on the adsorption capacity. Moreover, the lower initial concentration of phenol results in a slower diffusion of the pollutant, and accordingly, more active sites of the adsorbent remain. Hence, achieving breakthroughs takes more time, causing a delay in the saturated adsorption time (Iheanacho *et al.*, 2021; Rout, Bhunia, Dash, 2017). The adsorption capacity of GTX/AC adsorbent can be affected by various factors. One such factor is the initial concentration and pH level. In Fig. 8, it can be seen that the maximum adsorption capacity is achieved at the highest initial concentration of 500 mg/L and a pH of 6.35. When the pH level is below 8, the results indicate that as the initial concentration increases from 100 to 500 mg/L, the  $q_e$  value also increases. The results shown in Fig. (8) indicate that the effect of concentration is more considerable than the pH effect. According to the literature review, in each adsorption process, the contaminant solution's pH affects both the adsorbent's chemical properties (in this research: GTX/AC) and the adsorbate (Supong *et al.*, 2020). In this research, for pH>8, adsorbate and adsorbent have the same charge, therefore, this repulsion causes less adsorption of phenol in this range of pH, and the adsorption capacity has a decreasing trend. The phenol species has no charge at neutral pH, and because the GTX/AC adsorbent surface is positively charged, the adsorbent has a higher adsorption efficiency in this range.

The simultaneous effects of pH and adsorbent dosage on adsorption capacity are illustrated in Fig. 9. Results show that increasing the adsorbent dosage (from 5 to 20 gr) increased the available phenol adsorption sites, causing more phenol removal. Moreover, the maximum amount of adsorption capacity was obtained in higher adsorbent dosages. The Fig. 9 indicates that the maximum adsorption capacity happened at the highest adsorbent dosage (20 g) and pH= 2. At the low adsorbent dosage (5 g), the slope of the plot significantly changes by varying in the pH range of 3-8. The result shows an increase in the adsorption capacity in this pH range. However, with increasing adsorbent dosage at the lowest and highest levels of pH (ranges of pH < 2 and pH > 10), no noticeable change was observed in the slope of the plot.

Generally, the effect of pH appears more significant than the dosage. Accordingly, pH affects the surface charge of the adsorbent and the adsorbate molecules. Previous studies reported that for the phenol solution pH lower than the zero-point charge of the activated carbon adsorbent ( $\text{pH} < \text{pH}_{\text{pzc}}$ ), the surface of the activated carbon is positively charged (Sousa Ribeiro *et al.*, 2018; Hao *et al.*, 2018). Also, in the case of  $\text{pH} > \text{pH}_{\text{pzc}}$ , the surface of the activated carbon is negatively charged. The literature showed that the  $\text{pH}_{\text{pzc}}$  of activated carbon adsorbent is between 8 and 9 (Supong *et al.*, 2020; Sousa Ribeiro *et al.*, 2018; Beker *et al.*, 2010; Yadav *et al.*, 2020). When the activated carbon adsorbent surface has a positive charge within a pH range of 2 to 8, phenol remains undissociated. This creates an electrostatic attraction between phenol and the GTX/AC adsorbent surface, resulting in an increase in the adsorption capacity. Based on Fig. (9), for  $\text{pH} \leq 6.35$ , the decrease of phenol adsorption is gradual. Also, no noticeable adsorption capacity change was followed by varying doses from 5 to 20 gr at the lowest and highest pH levels ( $\text{pH} < 2$  and  $\text{pH} > 10$ ). Generally, the overall results described in this section indicate that the most vital parameters in the performance of the GTX/AC adsorbent are the initial concentration > pH > adsorbent dosage.

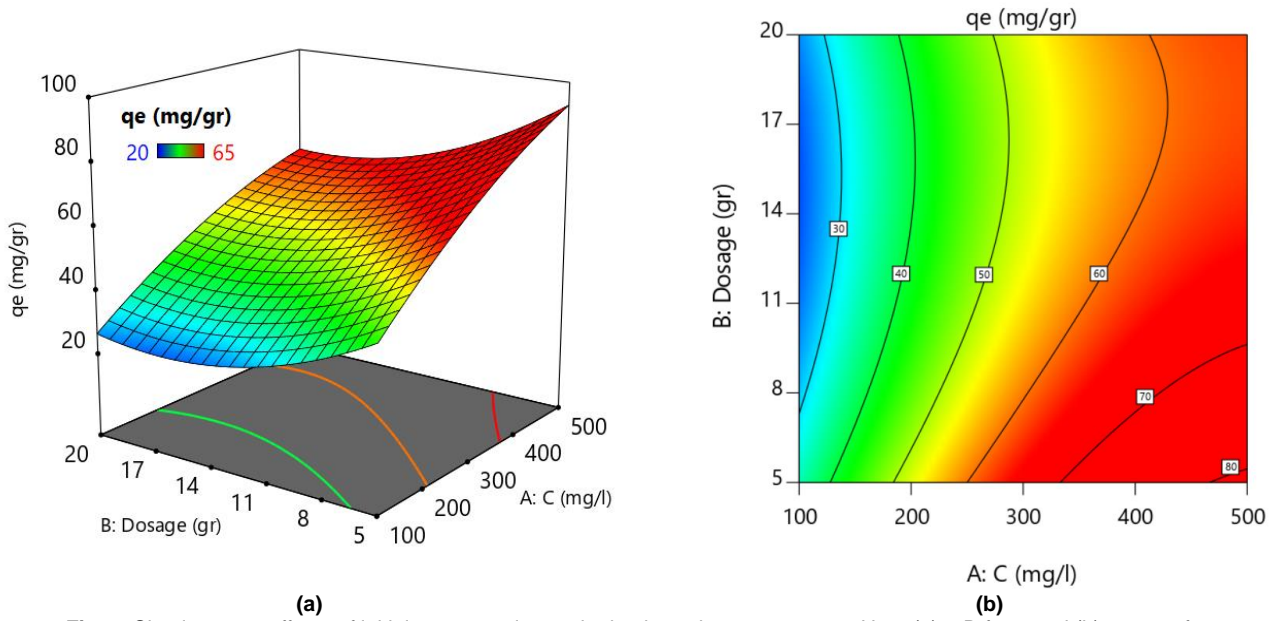


Fig. 7. Simultaneous effects of initial concentration and adsorbent dosage on  $q_e$  at pH=7, (a) 3-D form and (b) contour form.

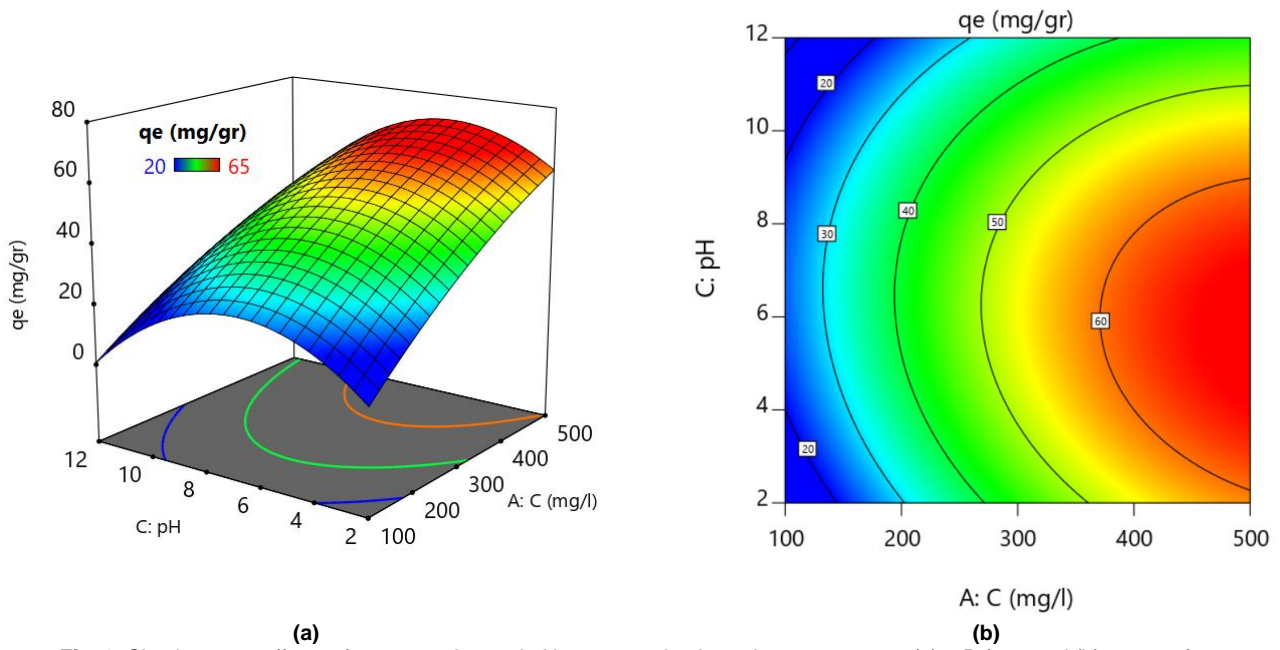


Fig. 8. Simultaneous effects of concentration and pH on  $q_e$  at adsorbent dosage=12.5 gr , (a) 3-D form and (b) contour form.

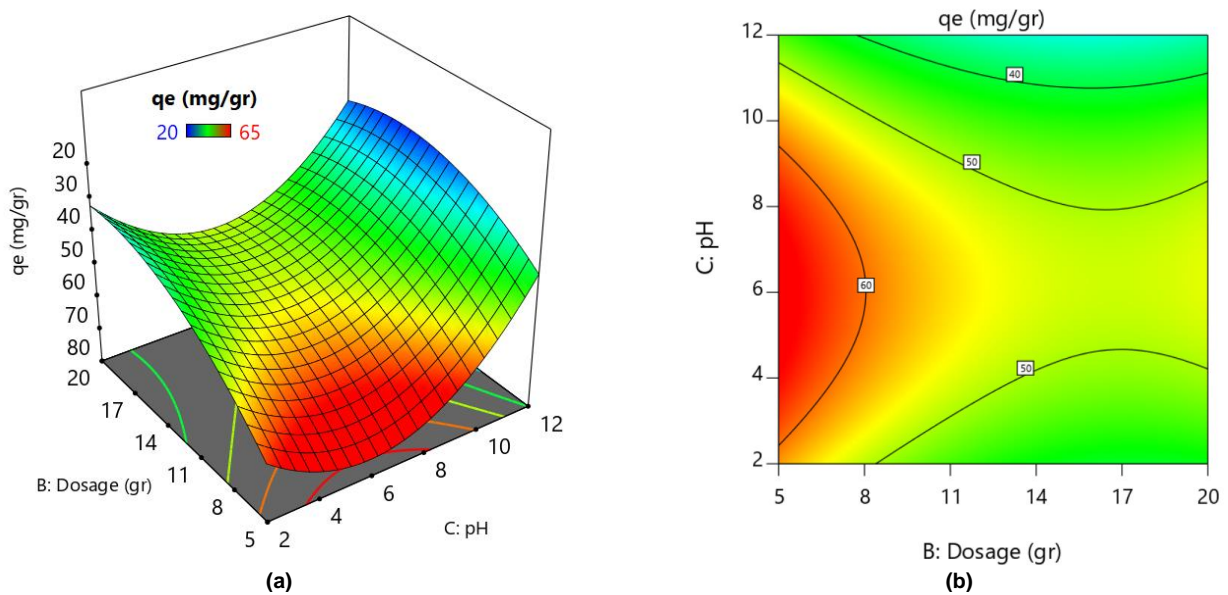


Fig. 9. Simultaneous effects of pH and adsorbent dosage on  $q_e$  at C= 300mg/L, (a) 3-D form and (b) contour form.

### 3.5. Optimization and validation of experiments

The present study performed a statistical optimization analysis to identify the most desirable combination of independent and dependent variables. These variables included the initial concentration, adsorbent dosage, pH, and maximum adsorption capacity. By utilizing a desirability function, the researchers could determine the optimal composition of these variables. Regarding the dependent variable (adsorption capacity), the initial concentration ranging from 100 mg/L to 500 mg/L, the adsorbent value in the 5-20 g range, and the  $6 \leq \text{pH} \leq 8$  were considered the target criteria in the optimization process. Among the 92 suggested options, the maximum adsorption capacity of 78.707 was obtained at the maximum level of desirability. Independent variables for reaching to this maximum adsorption capacity must be in this form: (1) the initial concentration = 458.8 mg/L; (2) adsorbent dosage = 5.5 g; and (3) pH= 7. A supplementary experimental test was conducted to verify the proposed optimized range of variables. This experimental test showed the maximum adsorption capacity value of 77.21, illustrating a 1.1% error from the proposed optimized range. Hence, the results show that the proposed model by RSM was in reasonable conformity with the experimental observations.

### 3.6. Breakthrough curve

The breakthrough curve is one of the most important results of the column test under the condition of flow velocity in the fixed bed (Rathour et al., 2022; Yu et al., 2022). Normally, the breakthrough curve has been used for column and fixed-bed studies to determine the adsorption performance of the sand column and adsorbent filter. To analyze the results, the dimensionless ratio  $C_t/C_0$  was used in Fig. 10, where  $C_0$  and  $C_t$  are the initial concentration and outlet concentration of the adsorbent, respectively. This curve shows the efficiency of the column, the volume of pollutants entering the column, the time of breakthrough and saturation of the bed or column, etc. The time when the  $C_t/C_0$  ratio exceeds 10% of the input concentration value is defined as the "breakthrough time". Also, the "saturation time" was considered when the  $C_t/C_0$  ratio exceeded 90% of the normalized volume (Rathour et al., 2022; Yu et al., 2022). In the present study, the ratio of the concentration of the adsorbed material at the outlet of the GTX/AC column to the initial concentration of phenol was plotted against time. From this curve, the column system's breakdown time and saturation time can be obtained. By utilizing the calculated times, it becomes possible to make estimations about the operation of the column system, the lifespan of the bed, and the time needed for the adsorbent to regenerate. Additionally, these calculated times can help determine if it is necessary to replace or reuse the column adsorbent and take appropriate measures accordingly. Based on the results (Fig. 10), the breakthrough and saturation times were 13.4 and 139.6 minutes, respectively. According to the Fig. 10, the replacement of GTX/AC after 75 minutes is suitable.

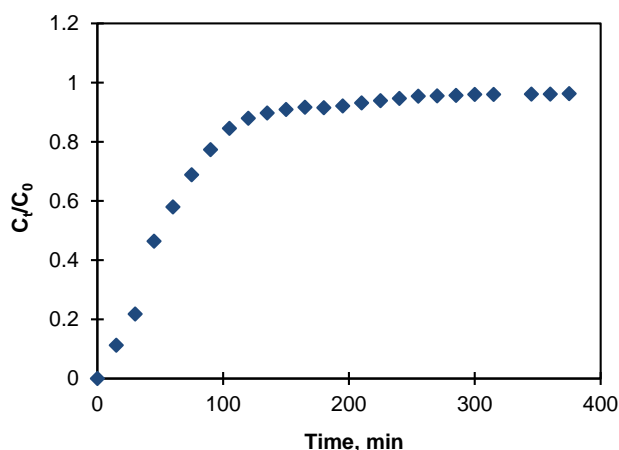


Fig. 10. Breakthrough curve under optimized condition (pH=7, C=458.8 mg/L, and dosage=5.5 g).

### 3.7. Removed phenol and removal efficiency in optimized condition

The "Amount of removed pollutant from groundwater" curve against time is depicted in Fig. 11. This figure show that how much phenol has

been removed from groundwater by the adsorbent under the optimal conditions during 75 minutes. Results revealed that the low adsorbent amount can adsorbed high amount of phenol from groundwater during process time. Based on the results, it can be concluded that 286 mg of phenol can be removing from about 0.94 L of groundwater during about 75 min.

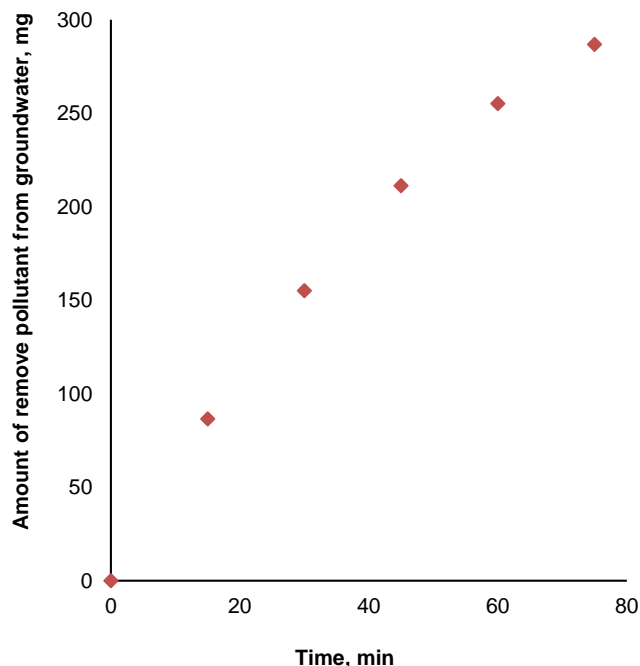


Fig. 11. Amount of removed pollutant from 0.94 L of groundwater at the optimized condition (pH=7, C=458.8 mg/L, and dosage=5.5 gr, Q=12.5 mL/min).

Also, Fig. 12 shows the amount of residual phenol in the solution (mg) and phenol removal efficiency (%) at the optimized condition. Based on the results, 0.94 L of polluted water can pass from the column during 75 minutes with flowrate equal to 12.5 mL/min. This 0.94 L had 431 mg of phenol (458.8 mg/L) at beginning. After passing this amount of water from column, 286 mg of phenol removed from water and only 145 mg of phenol remained. Fig. 12 shows 67% of removal efficiency for treatment of 0.94 L of groundwater during 75 minutes.

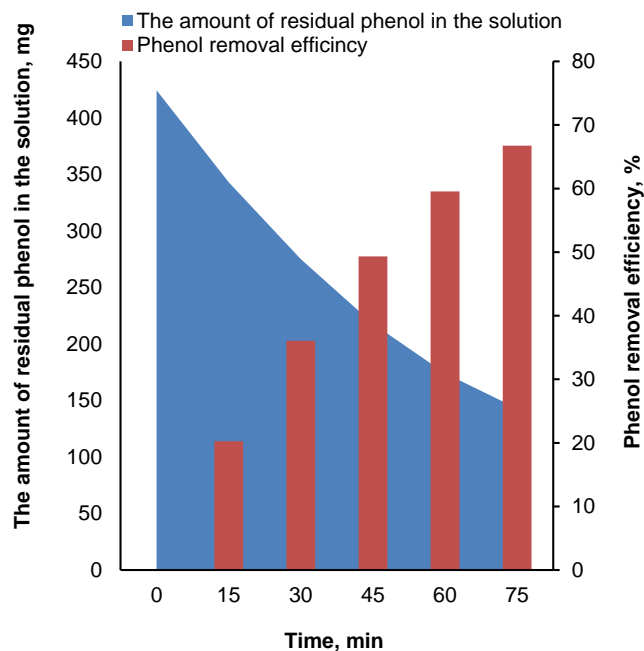


Fig. 12. The amount of residual phenol in the solution (mg) and Phenol removal efficiency (%) at the optimized condition (V=0.94 L, Q= 12.5 mL/min, pH=7, C=458.8 mg/L, and dosage=5.5 gr).

#### 4. Conclusions

In this study, a comprehensive test program was designed by RSM to determine the adsorption capacity of the GTX/AC adsorbent. The key factors that had the most impact on this system were the starting level of pollutants, the pH, and the amount of adsorbent used, in that order. The outcomes indicated that higher initial concentrations of pollutants lead to an increase in the capacity for adsorption. However, using a larger amount of adsorbent can actually decrease the adsorption capacity. The findings indicate that the adsorption capacity of the input contaminant solution is higher in the acidic and neutral pH ranges than in the upper neutral pH range. The investigations carried out in this research conclude that the GTX/AC adsorbent is a good choice for the adsorption of phenol from the groundwater. RSM is a powerful technique for modeling and optimizing processes that can be used for groundwater treatment. It is important to note that there are limitations to the present study. These include examining various flow rate effects, column geometry effects, and the effect of soil type. It is recommended that future studies investigate these limitations.

#### Author Contributions

Khatereh Ahmadi: Formal analysis, validation, writing - original draft preparation.

Farhad Qaderi: Supervision, data curation, conceptualization, methodology, investigation, writing - review and editing.

Mustapha Rahmaninezhad: Advisor, data curation, conceptualization, methodology.

Reza Shidpour: Advisor, data curation, conceptualization, methodology.

#### Conflict of Interest

The authors declare that they have no competing interests.

#### Acknowledgments

The authors would like to thank the Environmental Engineering laboratory at Babol Noshirvani University of Technology, Iran, for the valuable help in conducting experimental tests.

#### Data Availability Statement

The data are contained within the article.

#### References

- Abussaud B. et al. (2016) 'Sorption of phenol from waters on activated carbon impregnated with iron oxide, aluminium oxide and titanium oxide', *Journal of Molecular Liquids*, 213, pp. 351–359. doi: <https://doi.org/10.1016/j.molliq.2015.08.044>
- Allahkarami E. et al. (2023) 'Toward a mechanistic understanding of the adsorption behaviour of phenol onto a novel activated carbon composite', *Scientific Reports*, 13 (167), pp. 1–16. doi: <https://doi.org/10.1038/s41598-023-27507-5>
- Arida C.V.J. et al. (2016) 'Optimization of As(V) removal using chitosan-coated bentonite from groundwater using Box–Behnken design: effects of adsorbent mass, flow and initial concentration', *Desalination and Water Treatment*, 57 (40), pp. 18739–18747. doi: <https://doi.org/10.1080/19443994.2015.1094420>
- Beker U. et al. (2010) 'Adsorption of phenol by activated carbon: Influence of activation methods and solution pH', *Energy Conversion and Management*, 51(2), pp. 235–240. doi: <https://doi.org/10.1016/j.enconman.2009.08.035>
- Chen S. et al. (2022) 'Continuous silicic acid removal in a fixed-bed column using a modified resin: Experiment investigation and artificial neural network modeling', *Journal of Water Process Engineering*, 49, doi: <https://doi.org/10.1016/j.jwpe.2022.102937>
- Guo M. et al. (2019) 'Carbon nanotube-grafted chitosan and its adsorption capacity for phenol in aqueous solution', *Science of the Total Environment*, 682, pp. 340–347. doi: <https://doi.org/10.1016/j.scitotenv.2019.05.148>
- Han Y., Zhang Q., and Wu L. (2020) 'Influence on the adsorption of phenol on single-walled carbon nanotubes caused by NaCl and an electrostatic field in saline', *Desalination*, 477, pp. 114270. doi: <https://doi.org/10.1016/j.desal.2019.114270>
- Han Y. et al. (2018) 'Magnetic particles modification of coconut shell-derived activated carbon and biochar for effective removal of phenol

from water', *Chemosphere*, 211, pp. 962–969, doi: <https://doi.org/10.1016/j.chemosphere.2018.08.038>

Iheanacho O.C. et al. (2021) 'Packed bed column adsorption of phenol onto corn cob activated carbon: linear and nonlinear kinetics modeling', *South African Journal of Chemical Engineering*, 36, pp. 80–93. doi: <https://doi.org/10.1016/j.sajce.2021.02.003>

Khalatbary M. et al. (2022) 'Adsorption studies on the removal of malachite green by  $\gamma$ -Fe<sub>2</sub>O<sub>3</sub>/MWCNTs/Cellulose as an eco-friendly nanoadsorbent', *Biomass Conversion and Biorefinery*, 14(2), pp.1–19. doi: <https://doi.org/10.1007/s13399-022-02475-4>

Khataei B., Mokhtarani N., and Ganjidoust H. (2017) 'Removal of crude oil from soil using enhanced electrokinetic method by surfactants', *Sharif journal of civil engineering*, 33.2 (2.1), pp.107-114., doi: <https://doi.org/10.24200/J30.2017.4544>

Khataei B., Mokhtarani N., and Ganjidoust H. (2019) 'Numerical solution of the equation governing on bioelectrokinetic process in remediation of clayey soil contaminated with crude oil', *Modares civil engineering journal*, 19 (1), pp.155-167, doi: <http://mcej.modares.ac.ir/article-16-20184-en.html>

Koolivand H. and Shahbazi A. (2018) 'Statistical optimization and modeling of methylene blue adsorption onto graphene oxide in batch and fixed-bed column', *Avicenna Journal of Environmental Health Engineering*, 5(1), pp. 21–34, doi: <https://doi.org/10.15171/ajehe.2018.04>

Mandal A. et al. (2021) 'Fixed-bed column study for removal of phenol by neem leaves—experiment, MLR and ANN analysis', *Sustainable Chemistry and Pharmacy*, 23, pp.100514, doi: <https://doi.org/10.1016/j.scp.2021.100514>

Moghimi F. et al. (2020) 'An investigation on the adsorption behavior of Sb (III) on a cationic ion exchange resin in Fixed-bed column: experimental design and breakthrough curves modeling', *Journal of Advanced Materials and Processing*, 8(1), pp.30–45. Available at: <https://www.sid.ir/FileServer/JE/1011620200103.pdf> (15 April 2020).

Mohammadi S. Z., Darijani Z., and Karimi M. A. (2020) 'Fast and efficient removal of phenol by magnetic activated carbon- cobalt nanoparticles', *Journal of Alloys and Compounds*, 832, p.154942, doi: <https://doi.org/10.1016/j.jallcom.2020.154942>

Nowrouzi M., and Abyar H. (2021) 'A framework for the design and optimization of integrated fixed-film activated sludge-membrane bioreactor configuration by focusing on cost-coupled life cycle assessment', *Journal of Cleaner Production*, 296, p. 126557, doi: <https://doi.org/10.1016/j.jclepro.2021.126557>

Rathour R.K.S. et al. (2022) 'Sand coated with graphene oxide-PVA matrix for aqueous Pb<sup>2+</sup> adsorption: Insights from optimization and modeling of batch and continuous flow studies', *Surfaces and Interfaces*, 32, pp. 102115, doi: <https://doi.org/10.1016/j.surfin.2022.102115>

Rout P. R., Bhunia P., and Dash R. R. (2017) 'Evaluation of kinetic and statistical models for predicting breakthrough curves of phosphate removal using dolochar-packed columns', *Journal of Water Process Engineering*, 17, pp. 168–180, doi: <https://doi.org/10.1016/j.jwpe.2017.04.003>

Roy S., Das P., and Sengupta S. (2017) 'Treatability study using novel activated carbon prepared from rice husk: Column study, optimization using response surface methodology and mathematical modeling', *Process Safety and Environmental Protection*, 105, pp.184–193. doi: <https://doi.org/10.1016/j.psep.2016.11.007>

Shanmugaprakash M. et al. (2018) 'Biosorptive removal of Zn (II) ions by Pongamia oil cake (Pongamia pinnata) in batch and fixed-bed column studies using response surface methodology and artificial neural network', *Journal of Environmental Management*, 227, pp. 216–228, doi: <https://doi.org/10.1016/j.jenvman.2018.08.088>

Sharafi K. et al. (2019) 'Phenol adsorption on scoria stone as adsorbent - Application of response surface method and artificial neural networks', *Journal of Molecular Liquids*, 274, pp. 699–714, doi: <https://doi.org/10.1016/j.molliq.2018.11.006>

Sousa Ribeiro L. A. et al. (2018) 'Preparation, characterization, and application of low-cost açai seed-based activated carbon for phenol adsorption', *International Journal of Environmental Research*, 12, pp. 755–764. doi: <https://doi.org/10.1007/s41742-018-0128-5>

Supong A. et al. (2020) 'Experimental and theoretical insight into the adsorption of phenol and 2,4-dinitrophenol onto Tithonia diversifolia



- activated carbon', *Applied Surface Science*, 529, pp.147046, doi: <https://doi.org/10.1016/j.apsusc.2020.147046>
- Wang L (2006) 'Recommendations for design parameters for central composite designs with restricted randomization', *Submitt. to Fac. Virginia Polytech, Inst. State Univ. Partial fulfillment Requir. degree Dr. Philos.* pp. 20–60. Available at: <https://www.proquest.com/openview/0726c71f30ec02e58a22f3f5fc4d1dc4/1?pq-origsite=gscholar&cbl=18750&diss=y> (11 May 2006).
- Yadav N. et al. (2020) 'Adsorption and equilibrium studies of phenol and para-nitrophenol by magnetic activated carbon synthesised from cauliflower waste', *Environmental Engineering Research*, 25(5), pp. 742–752, doi: <https://doi.org/10.4491/eer.2019.238>
- Yu F. et al. (2022) 'Batch and continuous fixed-bed column adsorption of tetracycline by biochar/MOFs derivative covered with κ-carrageenan/calcium alginate hydrogels', *Journal of Environmental Chemical Engineering*, 10(3), p.107996. doi: <https://doi.org/10.1016/j.jece.2022.107996>